IV Journeys in Multiphase Flows (JEM2017)
March 27-31, 2017 - São Paulo, Brazil

PaperID: JEM-2017-0009

HEAT TRANSFER MODELING OF CONDENSATION IN UPWARD FLOW OF R-134a IN A 5-mm TUBE

Bernardo P. Vieira
Jader R. Barbosa Jr.
Polo - Research Laboratories for Emerging Technologies in Cooling and Thermophysics
Department of Mechanical Engineering, Federal University of Santa Catarina, Florianopolis, SC, Brazil
jrb@polo.ufsc.br

Abstract. *Condensation of vapors in vertical and inclined channels is encountered in a number of applications. In this paper, we present a mathematical model based on momentum and energy balances in annular flow (considering the superheated vapor and non-equilibrium vapor-liquid regions) to predict the heat transfer parameters associated with the condensation of R-134a in a 5-mm ID 950-mm long inclinable tube. The model results are compared with the experimental data of Barbosa et al.(2016), showing a good agreement.*

Keywords: *Condensation, Annular flow, Modeling.*

1. INTRODUCTION

Simulation of two-phase flows with condensation in vertical and inclined channels has several applications in the design of thermal systems. In reflux condensers (Hewitt *et al.*, 1994), understanding the physical nature of the *flooding* and *flow reversal* phenomena is crucial to devising accurate and reliable prediction methods. In refrigeration systems, tubings are sized so as to guarantee the oil return to the compressor sump and to avoid the refrigerant condensate return to the compressor (Tiandong *et al.*, 2012). In the particular case of in-tube condensation, a considerable number of models have been proposed to predict the frictional pressure gradient and the convection heat transfer coefficient in vertical and horizontal/inclined tubes (Liebenberg and Meyer, 2008; Lips and Meyer, 2011; Shah, 2016).

The objective of this study is to develop a mathematical model to predict the heat transfer and pressure drop in upflow condensation of refrigerants. The model results are compared with experimental data for R-134a condensation in a 5-mm ID 950-mm long inclinable tube (Hense, 2014; Barbosa *et al.*, 2016). The model consists of one-dimensional momentum and energy balances for unidirectional annular flow, considering the thermal non-equilibrium between the phases.

2. EXPERIMENTAL WORK

The experimental facility from which the experimental results were obtained is illustrated in Fig. 1. A detailed description of the setup is available in Barbosa *et al.* (2016). It consists of a mechanical vapor compression refrigeration loop equipped with an oil-free compressor. The test section (1 in Fig. 1) is illustrated in detain in Fig. 2. It is divided into three parts: inlet header, heat exchange region and outlet header. Temperatures and pressures are measured in the inlet and outlet headers. The heat exchange region consists of a countercurrent double pipe heat exchanger (950-mm long), whose internal tube is made from borosilicate glass (5 mm ID, 1-mm wall thickness). The annular gap is formed between the outer wall of the inner tube and the inner wall of a transparent acrylic resin (outer) duct. The internal diameter of the outer duct is 11 mm, resulting in a hydraulic diameter of 4 mm for the annular gap.

Superheated R-134a enters the inlet header with a 2°C superheat and mass flow rates ranging from 3 to 6 kg/h. Experiments were conducted at two different condensing pressures (830 and 1040 kPa). Through the annular gap, a counter flow of ethylene glycol (secondary fluid) is responsible for the R-134a condensation. The inlet temperature and the mass flow rate of the secondary fluid can be varied independently to control the condensation rate.

3. MODELING

A schematic diagram of the model geometry is shown in Fig.3. The refrigerant enters at the bottom of the test section with a prescribed pressure and a prescribed inlet superheating degree (superheated vapor). The refrigerant mass flow rate is known. The secondary fluid enters at the top of the test section, with a prescribed mass flow rate and inlet temperature.

As heat is transferred from the vapor to the secondary fluid, refrigerant condensation starts at the inner tube wall when it reaches the local saturation temperature. As a result, superheated vapor in the core region coexists for a certain length of tube with refrigerant condensate flowing as an annular film. In this non-equilibrium scenario, part of the heat exchanged with the secondary fluid is used to cool the vapor core, while the remainder is used to condense the vapor and sub-cool it to the inner wall temperature. As the flow evolves downstream, the superheating degree associated with the vapor core

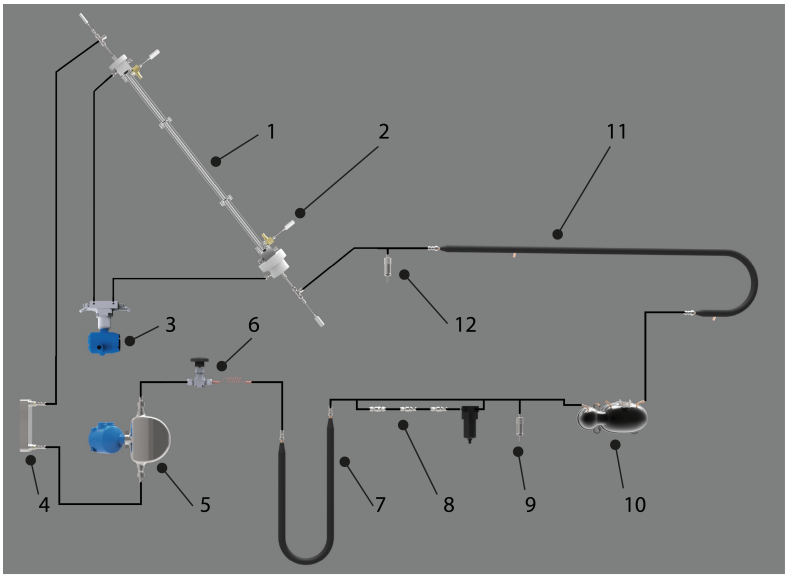

Figure 1. Experimental facility. Key to components: 1. Test section, 2. RTD Pt-100 transducer (fluid temperature), 3. Rosemont 3051S differential pressure transducer, 4. Alfalaval CBH16-9H Brazed plate condenser, 5. Micromotion CFMS010 mass flow meter, 6. Expansion (needle) valve and capillary tube, 7. Evaporator (electrical heater), 8. Filters, 9. Wika P-30-6 absolute pressure transducer, 10. Oil-free compressor, 11. Double-pipe heat exchanger. (Barbosa *et al.*, 2016).

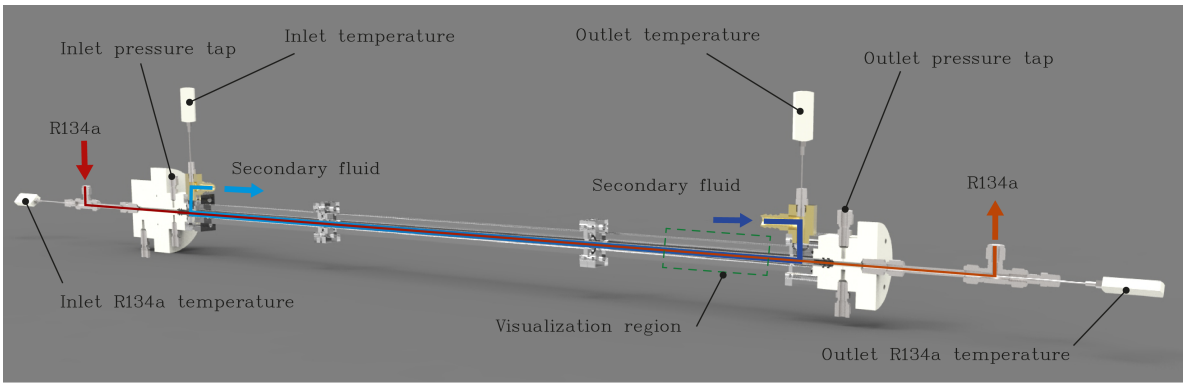

Figure 2. Test section of the experimental facility (Barbosa *et al.*, 2016).

decreases and the vapor eventually becomes saturated.

3.1 Single-Phase Region

In the single phase region, the pressure gradient is given by:

$$-\frac{dP}{dz} = \frac{2fG^2}{\rho_g D_i} + \rho_g g \sin\theta \tag{1}$$

where f is the Fanning friction factor and θ is the tube inclination from the horizontal, G is the mass flux, g is the acceleration of gravity, D_i is the inner tube diameter and ρ_g is the vapor density.

Upstream of the point at which vapor starts to condense, the energy balance equation is used to calculate the bulk enthalpy of the vapor as follows:

$$\frac{dh_g}{dz} = \frac{4q_w}{\pi G D_i^2} \tag{2}$$

where the wall heat transfer rate per unit length, q_w, is given by:

$$q_w = U\pi D(T_{sf} - T_g) \tag{3}$$

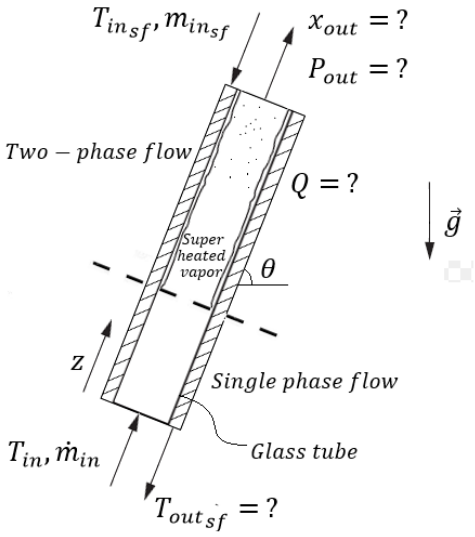

Figure 3. Geometry of the condensation problem.

and T_g is the local refrigerant bulk temperature (vapor only) and T_{sf} is the local bulk temperature of the secondary fluid. The overall thermal conductance per unit length is given by the sum of three terms as follows:

$$\frac{1}{U\pi D} = \frac{1}{h_{sf}\pi D_e} + \frac{\ln(D_i/D_e)}{2\pi k_{glass}} + \frac{1}{h_{wf}\pi D_i} \tag{4}$$

where the first, second and third terms on the right-hand side are the thermal resistances of the secondary fluid flow in the annular gap, glass tube and refrigerant flow, respectively. Since the secondary fluid flow was always laminar in the conditions examined in this study, the heat transfer coefficient h_{sf} was calculated using the Rohsenow and Hartnett correlation (Bergman *et al.*, 2011) for fully developed laminar flow for $D_e/D_i = 0.636$. The refrigerant flow is turbulent at the conditions studied here. Therefore, the heat transfer coefficient of the refrigerant flow in the single-phase region was computed using the Dittus-Boelter correlation (Bergman *et al.*, 2011).

With the above relationships, for a given temperature of the secondary fluid, the pressure and bulk vapor enthalpy as a function of distance are calculated, and the temperature of the tube wall can be determined at each step of the single phase flow domain until the point of refrigerant condensation is reached.

3.2 Two-Phase Region

In the two-phase flow region, annular flow is assumed to be established as soon as the vapor starts to condense at the tube wall. In this region, the pressure gradient is given by the following relationship (neglecting the acceleration term):

$$-\frac{dP}{dz} = \frac{4}{D}\tau_w + g[\rho_g\varepsilon + \rho_l(1-\varepsilon)]\sin\theta \tag{5}$$

where τ_w is the wall shear stress and ε is the void fraction.

A general relationship for the energy balance in the vapor core, taking into account the superheating of the bulk vapor is given by:

$$x_g\frac{dh_g}{dz} + h_g\frac{dx_g}{dz} = \frac{4q_I}{\pi G D_i^2} \tag{6}$$

where x_g is the vapor mass fraction and q_I is the interfacial heat transfer rate per unit length given by:

$$q_I = \pi\left(D - 2\delta\right)h_I\left(T_{sat} - T_g\right) \tag{7}$$

where δ is the annular film thickness (see Section 3.3), T_{sat} is the local saturation temperature (assumed at the interface) and h_I is the heat transfer coefficient between the bulk vapor and the interface, calculated using the Dittus-Boelter correlation.

The quality gradient as a function of distance is given by an energy balance in the liquid film as follows (neglecting the liquid film subcooling):

$$\frac{dx_g}{dz} = \frac{4\,(q_w - q_I)}{\pi G D_i^2 h_{lg}} \tag{8}$$

where h_{lg} is the enthalpy of vaporization of the refrigerant and q_w is given by:

$$q_w = U\pi D(T_{sf} - T_{sat}) \tag{9}$$

where the thermal conductance per unit length in the non-equilibrium region is given by:

$$\frac{1}{U\pi D} = \frac{1}{h_{sf}\pi D_e} + \frac{\ln(D_i/D_e)}{2\pi k_{glass}} + \frac{1}{h_{ann}\pi D_i} \tag{10}$$

where h_{ann} is the annular film heat transfer coefficient calculated as shown in Section 3.3 Note that as the bulk vapor superheating decreases, T_g approaches T_{sat} and q_I goes to zero asymptotically. Thus, in the saturated vapor region, the change in vapor quality is calculated via Eq. 8, with $q_I = 0$.

3.3 Annular flow model

In Eq. 5, relationships are needed to determine the wall shear stress and the void fraction, which is directly related to the liquid film thickness. Here, the triangular relationship (Hewitt and Hall-Taylor, 1970) between the liquid film mass flux, the wall shear stress and the liquid film thickness has been calculated using the approach of Cioncolini and Thome (2011). In this approach, the dimensionless film thickness is calculated by:

$$\delta^+ = \max\left(\sqrt{\frac{2\Gamma_{lf}^+}{R^+}}, 0.066\frac{\Gamma_{lf}^+}{R^+}\right) \tag{11}$$

where the dimensionless variables are given by:

$$\frac{\Gamma_{lf}^+}{R^+} = (1-e)(1-x)\frac{GD}{4\mu_l} \tag{12}$$

$$\delta^+ = \frac{\delta}{y^*} \tag{13}$$

$$y^* = \frac{\mu_l}{\rho_l V^*} \tag{14}$$

$$V^* = \sqrt{\frac{\tau_w}{\rho_l}} \tag{15}$$

In Eq. 12, e is the liquid entrained fraction in the gas core which, for simplicity, has been calculated assuming hydrodynamic equilibrium using the correlation of Cioncolini and Thome (2010) given by:

$$e = (1 + 13.18We_c^{-0.655})^{-10.77} \tag{16}$$

where the core Weber number is given by:

$$We_c = \frac{G_c D_c}{\sigma} \tag{17}$$

and the core mass flux, G_c, and diameter, D_c, are functions of the entrainment itself, therefore, an iteration process is needed to determine the liquid entrained fraction.

The wall shear stress, τ_w, is calculated based on a combination of momentum balances on the liquid film and vapor core to eliminate the pressure gradient, resulting in the following expression:

$$\tau_w = \frac{R^2 - R_I^2}{2R}\left[(\rho_l - \rho_c)g + \frac{2R^2\tau_i}{R_I(R^2 - R_I^2)}\right] \tag{18}$$

where R is the tube radius and $R_I = R - \delta$. The interfacial shear stress is calculated using the Wallis (1969) interfacial friction factor correlation as follows:

$$\tau_i = \frac{G_c^2}{2\rho_c} f_i \tag{19}$$

where ρ_c is the core density (a weighted average density based on the entrained fraction) and:

$$f_i = f_{gc}\left(1 + 360\frac{\delta}{D}\right) \tag{20}$$

$$f_{gc} = 0.079 Re_c^{-0.25} \tag{21}$$

$$Re_c = \frac{G_c D}{\mu_g} \tag{22}$$

where:

$$G_c = G_g + G_{LE} \tag{23}$$

and G_{LE} can be obtained from:

$$e = \frac{G_{LE}}{G_{LE} + G_L} \tag{24}$$

It should be noted that to start the iterative procedure to determine the liquid film thickness and the wall shear stress, an initial guess for the latter is obtained through the Friedel (1979) correlation.

After numerical convergence of the liquid film thickness is obtained, the two-phase flow heat transfer coefficient can be determined. In the present study, two methods specifically devised to calculate heat transfer in annular flows have been evaluated. Cioncolini and Thome (2011) proposed a correlation based on the liquid film turbulent eddy diffusivity as follows. If $10 \leq \delta^+ \leq 800$ then:

$$1 + \alpha_t^+ = \frac{h_{ann}\delta}{k_l} = 77.6 \times 10^{-3} t^{+0.90} Pr^{0.52} \tag{25}$$

Otherwise, if $\delta^+ \leq 10$, then

$$1 + \alpha_t^+ = \frac{h_{ann}\delta}{k_l} = 1 \tag{26}$$

The second method is the correlation proposed recently by Shah (2016), which considers three different heat transfer regimes in upflow condensation in inclined tubes. Regime I is one of unidirectional upflow and occurs when the following condition is satisfied:

$$J_g^* \geq 0.98(Z + 0.263)^{-0.62} \tag{27}$$

where J_g^* is the Wallis parameter (a dimensionless vapor velocity) given by:

$$J_g = \frac{Gx}{\sqrt{gD\rho_g(\rho_l - \rho_g)}} \tag{28}$$

and the empirical parameter Z is given by:

$$Z = \left(\frac{1}{x-1}\right)^{0.8} p_r^{0.4} \tag{29}$$

In Regime I, the heat transfer coefficient is given by:

$$h_{ann} = h_I = h_L \left(1 + \frac{3.8}{Z^{0.95}}\right) \left(\frac{\mu_l}{14\mu_g}\right)^{(0.0058+0.557p_r)} \tag{30}$$

Regime III occurs when:

$$J_g \leq 0.95(1.254 + 2.27Z^{1.249})^{-1} \tag{31}$$

and the heat transfer coefficient is calculated by:

$$h_{ann} = h_{Nu} = 1.32Re_l^{-\frac{1}{3}} \left[\frac{\rho_l(\rho_l - \rho_g)gk_l^3}{\mu_l^2}\right]^{\frac{1}{3}} \tag{32}$$

Regime II takes place when neither of the above criteria is satisfied. In this regime, the heat transfer coefficient for is given by:

$$h_{ann} = h_I + h_{Nu} \tag{33}$$

In addition to the annular flow methods presented above, a more general correlation for condensation in plain tubes due to Cavallini and Zecchin (1974) has been evaluated. The correlation is given by:

$$Nu = \frac{0.0994^{C_1} Re_L^{C_2} Re_{eq}^{1+0.875C_1} Pr_L^{0.815}}{(1.58lnRe_{eq} - 3.28)(2.58lnRe_{eq} + 13.7Pr_L^{2/3} - 19.1)} \tag{34}$$

where:

$$C_1 = 0.126Pr_L^{-0.448} \tag{35}$$

$$C_2 = -0.113Pr_L^{-0.563} \tag{36}$$

$$Re_{eq} = \phi^{8/7} Re_{lo} \tag{37}$$

where ϕ_{lo} can be obtained through Friedel's correlation.

In some of the experimental conditions evaluated here, flow regimes other than annular flow have been observed (e.g., slug flow) near the refrigerant outlet (top of the test section) as a result of a higher condensation rate. Therefore, it is expected that in these conditions, a more general correlation will perform better than methods devised specifically for annular flow.

With the values obtained with the correlations exposed, it is possible to determine the heat exchange and the amounts responsible for cooling the gas core and condensating the vapor near the interface. This process is repeated in each step until the gas core reaches the saturation temperature and regular two-phase flow starts. The process for solving the two-phase flow are the same used in the non-equilibrium state, the only difference being that all the heat is used to condensate the vapor. The same process is then repeated in each step until the end of the tube is reached. A simplified representation of the solving process of each step is shown in the flow chart on Fig. 4.

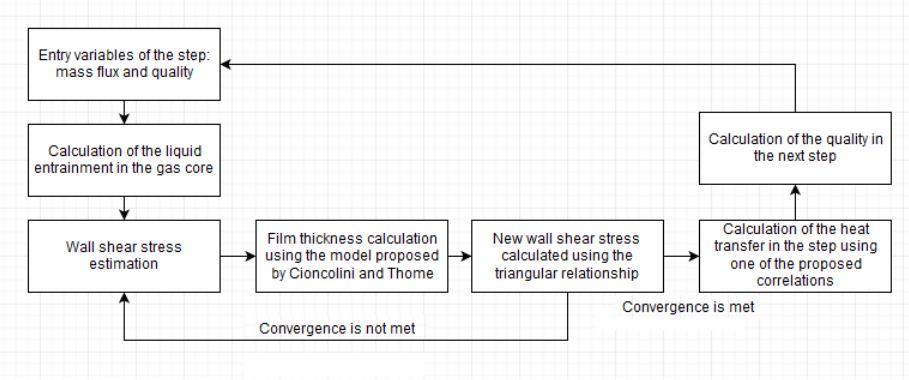

Figure 4. Solution process for each step of two-phase flow.

3.4 Secondary fluid flow and solution procedure

The energy balance in the secondary fluid flow is given by:

$$\frac{dh_{sf}}{dz} = -\frac{4q_w}{\pi G_{sf}(D_o^2 - D_e^2)} \tag{38}$$

which is solved coupled with the energy balance equation for the refrigerant flow. Since the outlet temperature of the secondary fluid is not known, an iterative calculation procedure is required to determine the secondary fluid temperature profile along the annular channel. A secondary fluid temperature profile is initially arbitrated so that the local heat transfer rate per unit length can be estimated and used in the integration of the energy balances. Thus, a new temperature profile is calculated and the process is repeated until convergence is obtained.

The tube was divided into 1,000 integration steps ($\Delta z = 0.95$-mm) and the equations were numerically integrated in Matlab using theRunge-Kutta method. The fluid properties were calculated via the CoolProp package. The input variables were the mass flow rates of both the R-134a (working fluid) and the secondary fluid, the refrigerant inlet temperature and pressure and the inlet temperature of the secondary fluid. In the experiments of **?** evaluated here, the refrigerant condensing pressure and the inlet superheat were 830 kPa and 2°C for all conditions.

4. RESULTS

The non-equilibrium state where the tube wall is below the saturation temperature is clearly shown in Fig. 5, where the tube wall is below the saturation temperature (assumed at the interface) and the vapor core still is superheated. Note that in this particular case (Test 5), the wall at the beginning of the tube is already below the saturation temperature, so the single phase flow part is virtually non-existent.

The model presented in Section 3 was used to simulate 11 different test conditions, using the three different methods to calculate the two-phase flow condensation heat transfer. The results for the overall heat transfer rate (measured experimentally through an energy balance in the secondary fluid) are shown in Tables 1, 2 and 3, which correspond to the methods of Cioncolini and Thome (2011), Shah (2016) and Cavallini and Zecchin (1974), respectively.

As mentioned before, the calculation method had a few limitations, mainly because the models proposed by Cioncolini and Thome (2011) and Shah (2016) were devised for annular flow along the whole tube, which was not the case in many of the test conditions (transitions to churn and slug flow have been observed in several runs). To avoid this problem, the correlation proposed by Cavallini and Zecchin (1974), which does not consider the flow pattern, was used to simulate the test conditions in which annular flow was not the only pattern observed. Even with these limitations, the results obtained were reasonably accurate for all correlations, with average differences from experimental and simulation results not surpassing 20%.

Test conditions numbered from 5 to 11 presented different flow patterns during considerable portions of the tube and, for that reason, Cavallini's correlation, which does not consider the flow pattern, presented the best reults for said tests, especially for the heat exchange calculation. However, all correlations, as previously mentioned, presented reasonably accurate results, with the average difference from the experimental and calculated results not surpassing 20% and the overall behaviour of the variables acting as expected. The same patterns can be observed in the results obtained for the secondary fluid exit temperature, in Tables 1, 2 and 3.

Both Cioncolini's and Shah's models presented approximately the same average deviation from the experimental results, while Cavallini's correlation presented better results overall. This further shows the influence of the different flow patterns present in the tube in the heat exchange, making the models assuming a specific flow pattern (annular) result in

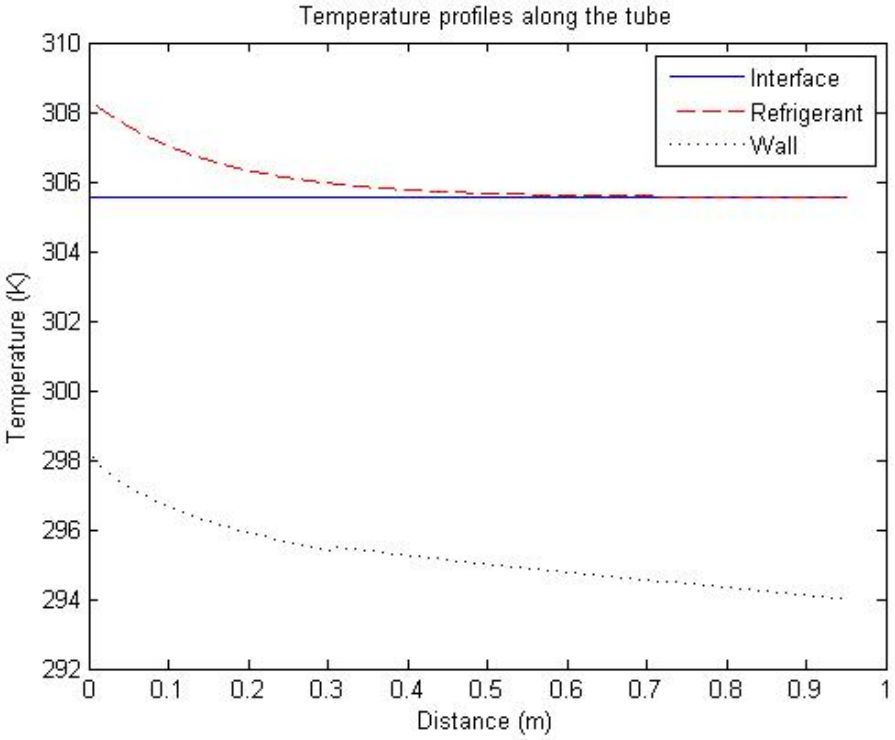

Figure 5. Temperature profiles of the interface, refrigerant and tube wall for Test 5.

Table 1. Heat exchange and secondary fluid exit temperature calculated using the heat exchange coefficient proposed by Cioncolini and Thome (2011).

Results - Cioncolini								
Test	$\dot{m}_r(kg/h)$	$Q_{exp}(W)$	$Q_{sim}(W)$	$Q_dif(\%)$	$T_{sf,exp}(^\circ C)$	$T_{sf,sim}(^\circ C)$	$T_{sf,dif}(^\circ C)$	x_{out}
1	5.056	40.67	51.46	26.53	24.45	26.41	1.96	0.75
2	5.053	57.87	74.11	28.06	22.19	22.73	0.54	0.69
3	5.026	81.43	95.17	16.87	19.29	19.67	0.38	0.62
4	5.046	90.62	98.69	8.90	18.71	18.88	0.17	0.60
5	4.926	106.01	120.32	13.49	15.64	16.06	0.42	0.49
6	5.064	126.40	162.29	28.40	10.28	12.00	1.72	0.33
7	5.142	142.99	184.93	29.33	6.83	8.51	1.68	0.25
8	5.142	155.82	186.04	19.39	6.38	7.34	0.96	0.24
9	5.142	156.18	185.37	18.69	6.61	7.53	0.92	0.25
10	5.142	165.62	186.62	12.68	5.58	5.97	0.39	0.21
11	5.142	179.36	203.50	13.46	2.92	3.33	0.41	0.13

values that overestimate the heat exchange inside the tube.

5. CONCLUSIONS

Ascending flow in a vertical tube was simulated using three different models previously proposed for heat exchange calculation. The method for calculating the film thickness and wall shear stress was the same for all cases. The model used demanded a low computational cost, due to the use of a simpler method of calculating the film thickness proposed by Cioncolini and Thome (2011). The wall shear stress was initially estimated using Friedel's correlation (1979), which was used along with the film thickness in the triangular correlation proposed by Hewitt and Hall-Taylor (1970), which resulted in a new wall shear stress, until convergence. The liquid entrainment in the gas core was calculated using the model proposed by Cioncolini and Thome (2011) and the heat exchange was calculated with one of the three mentioned models.

Two of the models used (Cioncolini's and Shah's) were proposed to simulate only annular flow, and the other model

Table 2. Heat exchange and secondary fludi exit temperature calculated using the heat exchange coefficient proposed by Shah (2016).

Results - Shah								
Test	$\dot{m}_r(kg/h)$	$Q_{exp}(W)$	$Q_{sim}(W)$	$Q_dif(\%)$	$T_{sf,exp}(^\circ C)$	$T_{sf,sim}(^\circ C)$	$T_{sf,dif}(^\circ C)$	x_{out}
1	5.056	40.67	52.38	28.79	24.45	26.57	2.12	0.75
2	5.053	57.87	73.24	26.56	22.19	22.90	0.71	0.68
3	5.026	81.43	96.42	18.41	19.29	19.70	0.41	0.61
4	5.046	90.62	99.91	10.25	18.71	18.90	0.19	0.60
5	4.926	106.01	121.12	14.26	15.64	16.08	0.44	0.49
6	5.064	126.40	161.80	28.00	10.28	11.98	1.70	0.33
7	5.142	142.99	183.28	28.18	6.83	8.46	1.63	0.25
8	5.142	155.82	184.20	18.22	6.38	7.30	0.92	0.25
9	5.142	156.18	183.60	17.56	6.61	7.49	0.88	0.26
10	5.142	165.62	184.26	11.25	5.58	5.94	0.36	0.22
11	5.142	179.36	199.52	11.24	2.92	3.29	0.37	0.14

Table 3. Heat exchange and secondary fludi exit temperature calculated using the heat exchange coefficient proposed by Cavallini and Zecchin (1974).

Results - Cavallini								
Test	$\dot{m}_r(kg/h)$	$Q_{exp}(W)$	$Q_{sim}(W)$	$Q_dif(\%)$	$T_{sf,exp}(^\circ C)$	$T_{sf,sim}(^\circ C)$	$T_{sf,dif}(^\circ C)$	x_{out}
1	5.056	40.67	57.10	40.41	24.45	26.74	2.29	0.77
2	5.053	57.87	76.44	32.09	22.19	23.42	1.23	0.71
3	5.026	81.43	98.87	21.42	19.29	20.02	0.73	0.65
4	5.046	90.62	99.31	9.59	18.71	19.04	0.33	0.64
5	4.926	106.01	107.76	1.65	15.64	15.76	0.12	0.55
6	5.064	126.40	145.34	14.99	10.28	11.31	1.03	0.40
7	5.142	142.99	164.62	15.13	6.83	7.84	1.01	0.33
8	5.142	155.82	164.96	5.86	6.38	6.83	0.45	0.33
9	5.142	156.18	164.49	5.32	6.61	7.03	0.42	0.34
10	5.142	165.62	163.54	1.26	5.58	5.68	0.10	0.31
11	5.142	179.36	176.84	1.41	2.92	3.03	0.11	0.24

(Cavallini's) was more generic, not considering the flow pattern in the heat exchange calculation. In most of the experimental conditions, flow patterns other than annular flow were present, resulting in considerable differences between the first two models and the results obtained experimentally. All three models, however, presented average differences not higher than 20%, with Cavallini's presenting the better results due to the other flow patterns in the tube.

6. ACKNOWLEDGEMENTS

This work was made possible through financial investment from the EMBRAPII Program (POLO/UFSC EMBRAPII Unit - Emerging Technologies in Cooling and Thermophysics). Financial support from Petrobras and CNPq (Grant No. 573581/2008-8 - National Institute of Science and Technology in Cooling and Thermophysics) is duly acknowledged.

7. REFERENCES

Barbosa, J.R., Ferreira, J.C.A. and Hense, D., 2016. "Onset of flow reversal in upflow condensation in an inclinable tube". *Experimental Thermal and Fluid Science*, Vol. 77, pp. 55–70.

Bergman, T.L., Lavine, A.S., Incropera, F.P. and DeWitt, D.P., 2011. *Fundamentals of Heat and Mass Transfer*. Wiley, seventh edition.

Cavallini, A. and Zecchin, R., 1974. "A dimensionless correlation for heat transfer in forced convection condensation". In *6th International Heat Transfer Conference*. Tokyo, pp. 309–313.

Cioncolini, A. and Thome, J.R., 2010. "Prediction of the entrained liquid fraction in vertical annular gasâĂŞliquid two-phase flow". *International Journal of Heat and Fluid Flow*, Vol. 36, pp. 293–302.

Cioncolini, A. and Thome, J.R., 2011. "Algebraic turbulence modeling in adiabatic and evaporating annular two-phase flow". *International Journal of Heat and Fluid Flow*, Vol. 32, pp. 805–817.

Friedel, L., 1979. "mproved friction pressure drop correlations for horizontal and vertical two-phase pipe flow". In *European Two-Phase Flow Group Meeting, Paper E2*. Ispra, Italy.

Hense, D., 2014. *Estudo experimental da limitação de escoamento em contracorrente na condensação de R-134a em tubos verticais e inclinados de pequeno diâmetro*. Master's thesis, Universidade Federal de Santa Catarina, Florianópolis, Brazil.

Hewitt, G.F. and Hall-Taylor, N.S., 1970. *Annular Two-Phase Flow*. Pergamon Press, Harwell, England, 1st edition.

Hewitt, G.F., Shires, G.L. and Bott, T.R., 1994. *Process Heat Transfer*. Begell House.

Liebenberg, L. and Meyer, J.P., 2008. "A review of flow pattern-based predictive correlations during refrigerant condensation in horizontally smooth and enhanced tubes". *Heat Transfer Engineering*, Vol. 29, pp. 3–19.

Lips, S. and Meyer, J.P., 2011. "Two-phase flow in inclined tubes with specific reference to condensation: A review". *International Journal of Multiphase Flow*, Vol. 37, pp. 845–859.

Shah, M.M., 2016. "Prediction of heat transfer during condensation in inclined plain tubes". *Applied Thermal Engineering*, Vol. 94, pp. 82–89.

Tiandong, G., Jang, J.Y., Do, S., Jeong, J.H. and Choi, B., 2012. "Development of suction pipe design criterion to secure oil return to compressor". In *International Refrigeration and Air Conditioning Conference at Purdue*.

Wallis, G.B., 1969. *One-Dimensional Two-Phase Flow*. McGraw-Hill.

8. RESPONSIBILITY NOTICE

The authors are the only responsible for the printed material included in this paper.